Medical Physics
The International Journal of Medical Physics Research and Practice

# Computer-aided diagnostic scheme for lung nodule detection in digital chest radiographs by use of a multiple-template matching technique

Qiang Li, Shigehiko Katsuragawa, and Kunio Doi

Citation: Medical Physics **28**, 2070 (2001); doi: 10.1118/1.1406517
View online: http://dx.doi.org/10.1118/1.1406517
View Table of Contents: http://scitation.aip.org/content/aapm/journal/medphys/28/10?ver=pdfcov
Published by the American Association of Physicists in Medicine

# Computer-aided diagnostic scheme for lung nodule detection in digital chest radiographs by use of a multiple-template matching technique

Qiang Li,[a] Shigehiko Katsuragawa, and Kunio Doi
*Department of Radiology, The University of Chicago, 5841 South Maryland Avenue, Chicago, Illinois 60637*

(Received 7 June 2001; accepted for publication 16 July 2001)

We have been developing a computer-aided diagnostic (CAD) scheme to assist radiologists in improving the detection of pulmonary nodules in chest radiographs, because radiologists can miss as many as 30% of pulmonary nodules in routine clinical practice. A key to the successful clinical application of a CAD scheme is to ensure that there are only a small number of false positives that are incorrectly reported as nodules by the scheme. In order to significantly reduce the number of false positives in our CAD scheme, we developed, in this study, a multiple-template matching technique, in which a test candidate can be identified as a false positive and thus eliminated, if its largest cross-correlation value with non-nodule templates is larger than that with nodule templates. We describe the technique for determination of cross-correlation values for test candidates with nodule templates and non-nodule templates, the technique for creation of a large number of nodule templates and non-nodule templates, and the technique for removal of nodulelike non-nodule templates and non-nodulelike nodule templates, in order to achieve a good performance. In our study, a large number of false positives (44.3%) were removed with reduction of a very small number of true positives (2.3%) by use of the multiple-template matching technique. We believe that this technique can be used to significantly improve the performance of CAD schemes for lung nodule detection in chest radiographs. 
[DOI: 10.1118/1.1406517]

Key words: pulmonary nodule, computer-aided diagnosis, chest radiograph, multiple-template matching

## I. INTRODUCTION

It has been reported that radiologists can fail to detect pulmonary nodules on chest radiographs in as many as 30% of positive cases.[1,2] Many of the lung cancers missed by radiologists were actually visible in retrospect on previous radiographs.[3] Therefore, we have developed a computer-aided diagnostic (CAD) scheme to assist radiologists in the detection of pulmonary nodules on digital chest radiographs.[4–9] With our current scheme, a major problem is the relatively large number of false positives, which constitutes a main difficulty in the clinical application of the CAD scheme for nodule detection. In this study, we developed a multiple-template matching technique to significantly reduce the number of the false positives in our CAD scheme. With the multiple-template matching technique, a large number of nodule templates and non-nodule (false positive) templates are first prepared. The maximum cross-correlation values with nodule templates and non-nodule templates for each of the test candidates are then determined, and are employed for distinguishing non-nodules from nodules, because a nodule is generally more similar to nodule templates than to non-nodule templates, and a non-nodule is more similar to non-nodule templates than to nodule templates. It is expected, therefore, that the maximum cross-correlation value of a nodule with nodule templates is generally greater than that with non-nodule templates, and vice versa.

## II. MATERIALS AND METHODS

### A. Materials

We used a database of 100 abnormal posteroanterior (PA) chest radiographs selected in the Department of Radiology, the University of Chicago Hospitals.[9] A total of 122 nodules were confirmed, based on the consensus of two radiologists and verified by CT scans or radiographic follow-up. The nodule diameter ranged from 4 to 27 mm (average, 13 mm). The digital images were obtained by digitizing of the chest radiographs with a Konica laser film scanner. The original digital image has a pixel size of 0.175 mm, a matrix size of $2000\times2000$, and a gray level range of 10 bits. Because nodules are relatively large in chest images, we reduced the matrix size of the digital images by a factor of 4. Consequently, the final image has a pixel size of 0.7 mm and a matrix size of $500\times500$. In addition to the main database previously mentioned, we employed a supplemental database, the Japanese Standard Digital Image Database,[10] solely for creation of nodule templates and for training of the multiple-template matching technique, but not for the verification of our CAD scheme with the multiple-template matching technique. The supplemental database is called the JSRT database hereinafter because it was developed by the Japanese Society of Radiological Technology (JSRT), and will be described later in detail.

Figure 1 shows the relationship between various data sets employed thereafter, and how they were created, where TP

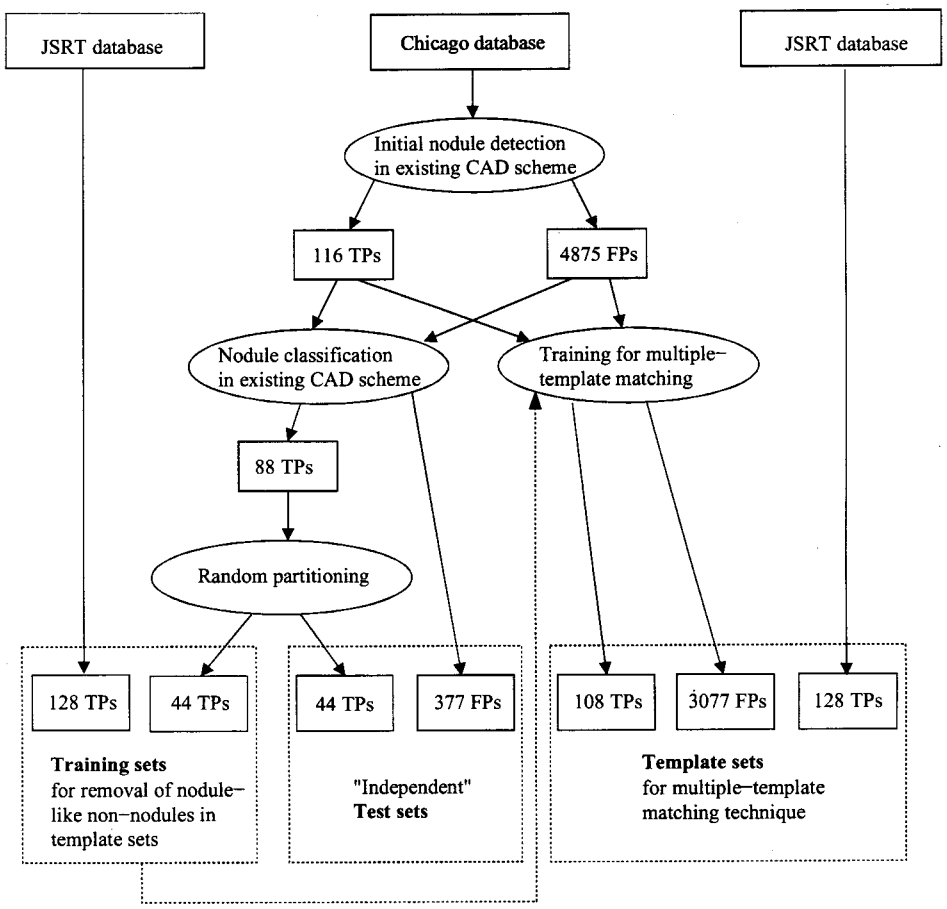


FIG. 1. Relationship between training sets, test sets, and template sets.

and FP imply true positive (nodule) and false positive, respectively. With our current CAD scheme, 116 nodules and 4875 false positives were initially detected from the 100 chest images in the main Chicago database. A rule-based classification technique was then applied to reduce the number of false positives,[9] with which we obtained 88 nodules and 377 false positives. The 88 nodules were randomly partitioned into two sets of equal size. One of which (44 nodules), plus the 128 nodules from the JSRT database, was called a training set and was employed to train the multiple-template matching technique, that is, for selection of appropriate templates. The other set (44 nodules) and the 377 false positives were called test sets and were used to test the technique. It is important to ensure that there is no overlap between the training sets and test sets, otherwise the experimental results for the technique will be biased. On the other hand, the 116 nodules and 4875 false positives detected initially by our CAD scheme were also used as initial nodule templates and initial non-nodule templates, respectively, from which 108 nodules and 3077 false positives (together with 128 nodules from the JSRT database) were selected as final templates by a training process, i.e., by eliminating nodule-like false positives and false-positive-like nodules. Although a test candidate in the test sets may be included in the template sets, the corresponding template was temporarily excluded from the template sets when computing the cross-correlation values between the test candidate and the template sets, as will be described later in detail. It should be noted that the 377 false positives in the test candidate sets survived our rule-based tests; therefore, they are considered as ''difficult'' false positives, which are similar to nodules.

### B. Summary of the current CAD scheme based on rule-based tests

First of all, the lung areas in PA chest images were segmented by use of the delineated ribcage edges, lung top, and diaphragm,[11,12] and were employed for the subsequent processing of the CAD scheme. A difference image was then obtained by subtraction of a nodule-suppressed image (by use of a smooth filter) from a nodule-enhanced image (by use of a matched filter), so that the complicated background structure could be reduced, and thus nodules could be more conspicuous. Next, a multiple thresholding technique was used for detection of initial nodule candidates whose effective diameter and degree of circularity were equal or greater than 6.5 mm and 0.65, respectively. For the Chicago database of 100 abnormal chest images, a total of 116 (out of 122) nodules and 4875 false positives were identified as initial nodule candidates.

A region growing technique[5,6] was applied to both the difference image and the original image at the locations of initial nodule candidates, for accurate segmentation of nodule candidates from background in each of the two images.

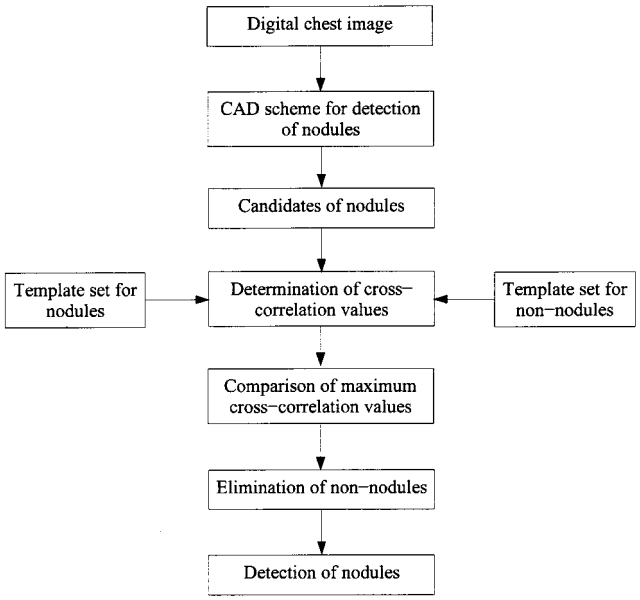


FIG. 2. Overall scheme for the multiple-templates matching technique.

Various features, such as the effective diameter, contrast, degree of circularity, degree of irregularity, edge gradient, slope of circularity, slope of irregularity, and slope of diameter, were then determined from each of the grown regions, and employed for distinction between nodules and false positives by a rule-based classification technique.[9] After this step, most nodules, 88 (75.9%) out of 116, were retained, and most false positives, 4498 (92.3%) out of 4875, were eliminated; thus, 377 false positives remained.

### C. Overall scheme of the multiple-template matching technique for reduction of false positives

Figure 2 shows the overall scheme for the multiple-template matching technique. First of all, the CAD scheme for nodule detection was applied for determination of nodule candidates. For each of the nodule candidates, we then employed a cross-correlation technique to calculate the cross-correlation values with the nodule template set and with the non-nodule template set. Finally, two maximum cross-correlation values obtained with the nodule template set and with the non-nodule template set were determined, and employed to eliminate false positives (non-nodules) in our CAD scheme if the maximum cross-correlation value with the non-nodule templates was larger than that with the nodule templates.

In order to apply the multiple-template matching technique, it is necessary to create two multiple-template sets, i.e., one with a large number of nodule templates and another with a large number of non-nodule templates. In this study, we used the initial nodule candidates (116 nodules and 4875 non-nodules) reported by our CAD scheme as initial templates, which were small regions of interest (ROIs) of 36 $\times$ 36 pixels centered at the locations of the initial nodule candidates. Each of the nodule templates was right/left reversed, scaled (minified or magnified), and rotated to increase the number of nodule templates. Eight non-nodule-like nodule templates (atypical nodules such as very subtle nodules overlapping ribs) were carefully identified as inappropriate nodule templates, and thus excluded from the nodule template set. Similarly, each of the non-nodule templates was right/left reversed, and rotated to increase the number of non-nodule templates. Many (1798) non-nodule templates that had a similar appearance as nodules were then systematically removed from the non-nodule template set by use of a training sets, as will be discussed later in detail, because the presence of these nodule-like non-nodule templates can considerably degrade the performance of the multiple-template matching technique. We did not scale the non-nodule templates, because we had a relatively large number of non-nodule templates, and also because the templates obtained by use of scaling were slightly obscured. However, the scaled nodule templates were used even though they were slightly obscured, because the number of nodules was very limited in this study. After the removal of non-nodule-like nodule templates and nodule-like non-nodule templates, we obtained 108 nodule templates in the nodule template set, and 3077 non-nodule templates in the non-nodule template set. Figures 3 and 4 show typical examples of nodule templates and non-nodule templates, respectively. It is apparent in Figs. 3 and 4 that nodule templates and non-nodule templates are quite different in appearance, and are thus the basis for distinction between nodules and non-nodules.

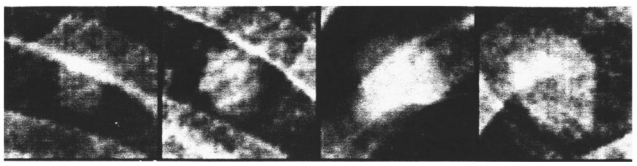

FIG. 3. Examples of nodule templates which are corrected for background trend.

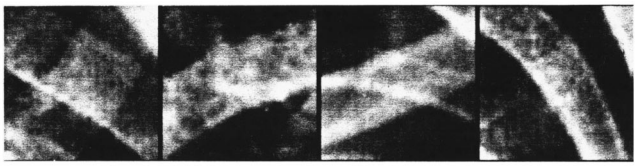

FIG. 4. Examples of non-nodule templates which are corrected for background trend.

### D. Determination of maximum cross-correlation values between a test candidate and the template sets of nodules and non-nodules

If a test candidate was included in the template sets when we calculate the cross-correlation values between the test candidate and the template sets, the corresponding template and its right/left reversed, scaled, and rotated templates would not be used for the determination of the cross-correlation value with the test candidate. Before the actual calculation of the cross-correlation value between a template and a test candidate, a preprocessing step was utilized for

correction of the background trend included in a template and test candidate. The background trend in the template (or test candidate) was represented by a two-dimensional (surface) linear function, and the three coefficients of the linear function were determined by a least square method. The estimated surface function was then subtracted from the original image of the template (or the test candidate) to provide a background-trend corrected image.

While a template had a matrix size of $36\times36$ pixels, a test candidate was a small ROI of $40\times40$ pixels centered at the location of nodule candidates in the test sets. In order to determine the cross-correlation value between a template $A$ and a test candidate $B$, we moved the template $A$ inside the test candidate $B$ for a maximum shift distance of 4 pixels in both horizontal and vertical directions, and a cross-correlation value $C_{i,j}$ was calculated at each shift vector $(i,j)$ by the equation:

$$C_{i,j}^2=\frac{1}{MN}\sum_{m=1}^{M}\sum_{n=1}^{N}\frac{\{A(m,n)-\overline{A}\}\{B_{i,j}(m,n)-\overline{B}\}}{\sigma_A\sigma_B},$$

$$i,j\in\{0,1,2,3,4\},$$

where $\overline{A}$ and $\sigma_A^2$ are the mean and variance of the pixel values in the template $A$, respectively, $\overline{B}$ and $\sigma_B^2$ are the mean and variance of the pixel values in a $36\times36$ subregion, $B_{ij}$, of the test candidate $B$ at a shift vector $(i,j)$, respectively, and $M$ and $N$ are the width and height of the template, respectively (both of them are 36 in this study). The mean and variance of the pixel values in regions $A$ and $B_{i,j}$ are defined by the following equations:

$$\overline{A}=\frac{1}{MN}\sum_{m=1}^{M}\sum_{n=1}^{N}A(m,n),$$

$$\overline{B}=\frac{1}{MN}\sum_{m=1}^{M}\sum_{n=1}^{N}B_{i,j}(m,n),$$

$$\sigma_A^2=\frac{1}{MN}\sum_{m=1}^{M}\sum_{n=1}^{N}\{A(m,n)-\overline{A}\}^2,$$

$$\sigma_B^2=\frac{1}{MN}\sum_{m=1}^{M}\sum_{n=1}^{N}\{B_{i,j}(m,n)-\overline{B}\}^2.$$

The largest cross-correlation value among all shift vectors $(i,j)$ was then determined as the cross-correlation value between the template and the test candidate. Next, we computed the cross-correlation values for the test candidate with all of the nodule templates, and we determined the maximum cross-correlation value, and employed it as a unique feature of the test candidate, which indicates the extent of the resemblance to the nodule. Similarly, the maximum cross-correlation value for the test candidate with the non-nodule template set was determined and used as another unique feature of the test candidate, which indicates the extent of the resemblance to the non-nodule. These two features for the candidates in the test sets were then employed for distinguishing false positives from nodules, when the maximum cross-correlation value with the non-nodule templates was larger than that with the nodule templates.

### E. Creation of nodule templates and non-nodule templates

A key factor for the success of the multiple-template matching technique is the number of templates available for nodules and non-nodules. In this study, we employed as original templates the 108 nodules and 3077 non-nodules in the Chicago database, and 128 nodules in the JSRT database. We then utilized the following three methods to increase the number of templates in this study:

(1) right/left reversing of a template to create a mirror template,
(2) scaling of a template by three different factors of 0.6, 0.8, and 1.2, and
(3) rotation of a template by two different angles, $-10$ and $+10$ degrees.

In order to obtain a scaled template, instead of scaling the original template, we scaled the entire image by a specific scaling factor, from which we then obtained the scaled template of $36\times36$ pixels at the appropriate location. Similarly, for creation of a rotated template, the entire image was first rotated at the center of the original template, and the rotated template of $36\times36$ pixels was then created from the rotated image. The right/left reversing enables a template in the right lung to be useful in the left lung and vice versa, and it doubles the number of templates. The scaling and the rotation in this study increased the number of templates by factors of 4 and 3, respectively, and thus the total number of templates can be increased 24 times by a combination of all of these methods. We found that the increase of templates by use of right/left reversing, scaling, and rotation can significantly improve the separation between the nodules and non-nodules in the test sets, when the two maximum cross-correlation values with the nodule template set and non-nodule template set were employed as features.

Another important parameter for the multiple-template matching technique is an appropriate choice of the matrix sizes for the templates and the test candidates. In this study, we examined the effect of various matrix sizes ranging from $24\times24$ pixels to $48\times48$ pixels on the overall performance. We found that the best results were obtained when the matrix sizes for the templates and the test candidates were $36\times36$ pixels (approximately $25\times25$ mm$^2$) and $40\times40$ pixels ($28\times28$ mm$^2$), respectively. Therefore, the matrix size of the templates used in this study was determined as $36\times36$ pixels.

### F. Elimination of nodule-like non-nodules in non-nodule template set

Figure 5 illustrates four non-nodule templates that resembled nodules in appearance. It is important to note that these nodule-like non-nodule templates significantly impair the performance of the multiple-template matching tech-

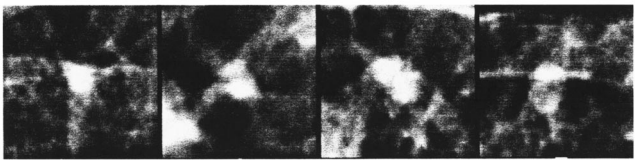

FIG. 5. Examples of nodule-like non-nodule templates.

nique, and thus should be eliminated in order to achieve a good performance for the multiple-template matching technique. We employed the training sets, the 44 nodules in the Chicago database and 128 nodules in the JSRT database, to achieve this task.

The JSRT database included 128 chest images with solitary lung nodules, which were selected from a total of 154 nodules cases in the Japanese Standard Digital Image Database developed by the Japanese Society of Radiological Technology.[10] We eliminated 26 nodule cases from the JSRT database, each of which contained a nodule with a subtlety rating score of either 1 or 5, corresponding to an extremely subtle nodule or an obvious nodule, respectively. The original chest images were digitized with a 0.175 mm pixel size, a matrix size of $2048\times2048$, and 12-bit gray levels. In this study, the matrix size was reduced to $512\times512$ by subsampling of the original image data by a factor of 4, and the number of gray levels was decreased to 10 bits, in order to be consistent with the chest images in the main database. The 128 nodules in the JSRT database together with the 108 nodules in the main database were used as the nodule template set for verification of the multiple-template matching technique. The 128 nodules were also employed for training of the multiple-template matching technique, namely, for the removal of nodule-like non-nodule templates.

For each of the 128 nodules, 20 non-nodule templates which provided the 20 largest cross-correlation values with the nodule were considered here to be nodule-like non-nodules, and were eliminated from the 4875 original templates in the initial non-nodule template set. A total of 1338 original non-nodule templates (and their mirror, scaled, and rotated templates) were thus removed, and 3537 original non-nodule templates remained in the non-nodule template set. Only 1338 unique non-nodule templates were actually eliminated (less than the theoretical maximum of $128\times20$) because each non-nodule template can be in the top 20 matches for more than one training nodule. Similarly, the 44 nodules in the Chicago training set were employed for further elimination of nodule-like non-nodules from the 3537 original templates. We thus again eliminated 460 original non-nodule templates (and their mirror, scaled, and rotated templates), and finally, 3077 original templates were left in the non-nodule template set. We removed a total of 1798 original templates from the initial non-nodule template set by employing the 128 nodules in the JSRT database and the 44 nodules in the Chicago database altogether.

Figure 6 shows the relationship between the maximum cross-correlation values with the nodule templates and non-nodule templates for the 44 nodules in the test sets, before

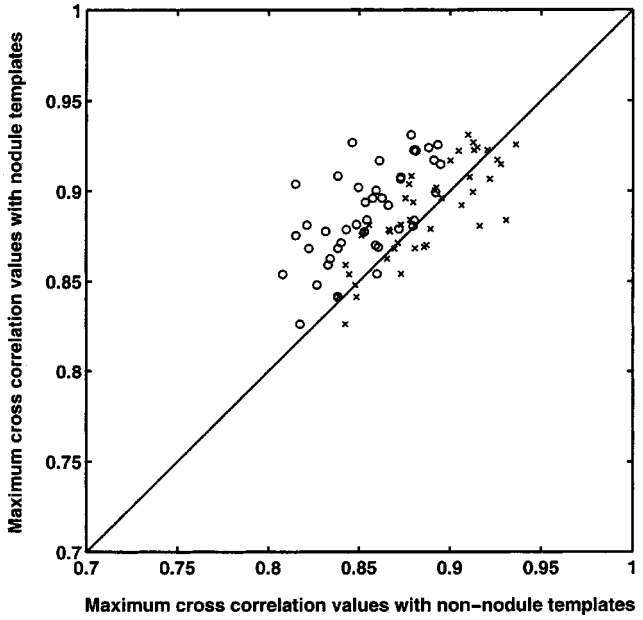


FIG. 6. Relationship between the maximum cross-correlation values with nodule templates and non-nodule templates, for the 44 nodules in the test sets, before (x's) and after (circles) the elimination of nodule-like non-nodule templates. There were 5664 templates in the nodule template set, and 29 250 and 18 462 templates in the non-nodule template set, respectively, before and after the elimination of nodule-like non-nodule templates.

(indicated by x's) and after (indicated by circles) the removal of the nodule-like non-nodule templates. The nodule template set used in Fig. 6 was composed of 5664 $(24\times236)$ templates, which included the 108 nodules in the main database and the 128 nodules in the JSRT database, and their mirror templates, scaled templates, and rotated templates. The non-nodule template set contained 29 250 $(6\times4875)$ templates and 18 462$(6\times3077)$ templates, respectively, before and after the removal of the nodule-like non-nodule templates, which included the original non-nodule templates, their mirror templates, and rotated templates. It is apparent in Fig. 6 that most nodules are moved significantly to the left by elimination of the nodule-like non-nodule templates, and that all but one nodule are located above the diagonal line.

It should be noted that the elimination of nodule-like non-nodule templates would also affect the non-nodules in the test sets. Figure 7 shows the relationship between the maximum cross-correlation values with the nodule templates and non-nodule templates, for one half (189) of the 377 non-nodules in the test sets, before (indicated by x's) and after (indicated by dots) the elimination of the non-nodule templates. Only half of the non-nodules are shown in Fig. 7 for a clearer display. The nodule template set and non-nodule template set used in Fig. 7 are the same as those employed in Fig. 6. It is apparent in Fig. 7 that, although some of the 377 non-nodules moved to the left as did the nodules in Fig. 6, many non-nodules still remain below the diagonal line after the elimination of the nodule-like non-nodule templates. These findings imply that, after elimination of nodule-like non-nodule templates, we can distinguish the false positives (non-nodules) below the diagonal line in Fig. 7 from the

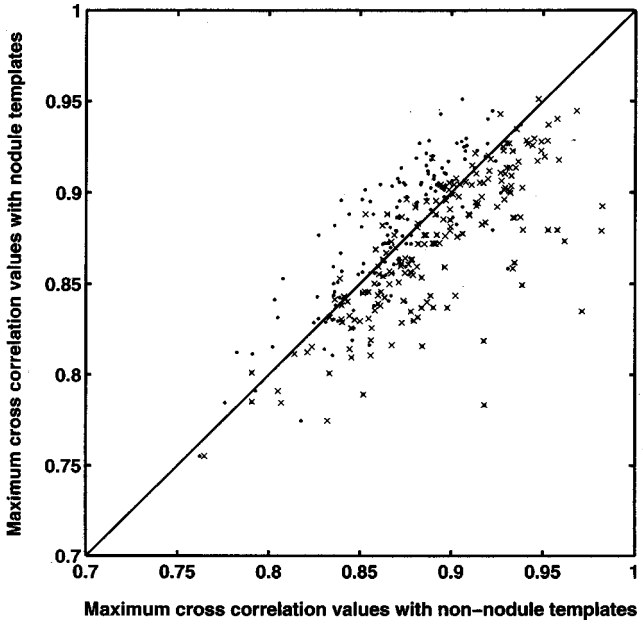


FIG. 7. Relationship between the maximum cross-correlation values with nodule templates and non-nodule templates, for half (189) of the 377 non-nodules in the test sets, before (x's) and after (dots) the elimination of nodulelike non-nodule templates. There were 5664 templates in the nodule template set, and 29 250 and 18 462 templates in the non-nodule template set, respectively, before and after the elimination of nodule-like non-nodule templates.

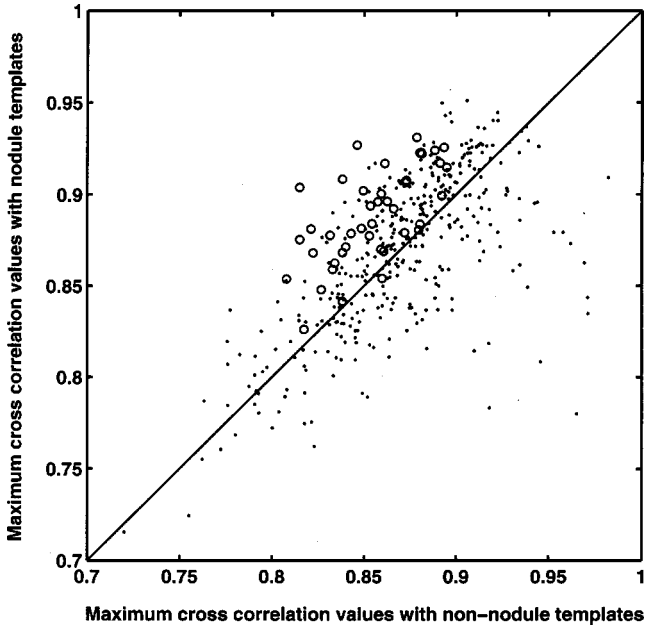


FIG. 8. Relationship between the maximum cross-correlation values with 5664 nodule templates and 18 462 non-nodule templates, for 44 nodules (circles) and 377 non-nodules (dots) in the test sets, after the elimination of nodule-like non-nodule templates in a validation test.

nodules in Fig. 6, because nearly all of the nodules are located above the diagonal lines.

### G. Results

With the 5664 nodule templates and 18 462 non-nodule templates after the elimination of nodule-like non-nodules, a validation test was conducted based on the 44 nodules and 377 non-nodules in the test sets. It should be noted that the 44 nodules and 377 non-nodules have not been utilized for training of the multiple-template matching technique, i.e., for elimination of either nodule-like non-nodules or non-nodule-like nodules in the template sets, although they were shown in Figs. 6 and 7 to demonstrate the effect of removing nodule-like non-nodule templates. Figure 8 shows the relationship between the maximum cross-correlation values with the 5664 nodule templates and 18 462 non-nodule templates for the 44 nodules and 377 non-nodules in the test sets. It is apparent in Fig. 8 that a significant distinction can be made between the nodules and false positives (non-nodules) based on the two maximum cross-correlation values. For example, if the diagonal line is used as a threshold, namely, if candidates located above the diagonal line are accepted as nodules, then we can eliminate 167 (44.3%) false positives from the 377 non-nodules with a reduction of only one (2.3%) true nodule. This actually constitutes a significant improvement of our CAD scheme because many of the 377 false positives are similar to nodules in appearance, and are thus considered as ''difficult'' false positives.

An interesting issue is the extent to which the results would be affected if the test set was excluded from, and thus independent of, the template set. Although it is difficult to estimate such influence in this study, we anticipate that the technique may be degraded significantly if the test set was excluded from the template set, especially at this stage where only a very limited number of nodule templates are available. In other words, excluding the test set has less effect as we increase the number of total available nodule templates. Further study with a large number of cases would be required in the future to accurately examine the effect of excluding the test set from the template set.

### H. Conclusion

We developed a multiple-template matching technique for distinction of false positives from nodules in our CAD scheme. After careful removal of a few non-nodule-like nodule templates and a large number of nodule-like non-nodule templates, a large fraction of false positives (44.3%) can be removed with a reduction of a very small number of true positives (2.3%) by use of the multiple-template matching technique. We believe that this technique has the potential to improve significantly the performance of our CAD scheme for nodule detection in digital chest radiographs.

## ACKNOWLEDGMENTS

This work was supported by USPHS Grant Nos. CA62625 and CA64370. The authors are grateful to E. Lanzl for improving the manuscript and to E. A. Ruzich for her secretarial work. K. Doi and S. Katsuragawa are shareholders of R2 Technology, Inc., Los Altos, CA, and K. Doi is a shareholder of Deus Technologies, Inc., Rockville, MD. It is the policy of the University of Chicago that investigators

disclose publicly actual or potential significant financial interests that may appear to be affected by research activities.

[a]Electronic mail:lqiang@kurt.bsd.uchicago.edu

[1] J. V. Forrest and P. J. Friedman, ''Radiologic errors in patients with lung cancers,'' West. J. Med. **134**, 485–490 (1981).
[2] D. P. Naidichi, E. A. Zerhouni, and S. S. Siegelman, *Computer Tomography of Thorax* (Raven, New York, 1984), pp. 171–199.
[3] J. R. Muhm, R. S. Miller, R. S. Fontana, D. R. Sanderson, and M. Uhlenhopp, ''Lung cancer detected during a screening program using four-month chest radiographs,'' Radiology **148**, 609–615 (1983).
[4] M. L. Giger, K. Doi, and H. MacMahon, ''Image feature analysis and computer-aided diagnosis in digital radiography. 3. Automated detection of nodules in peripheral lung fields,'' Med. Phys. **15**, 158–166 (1988).
[5] M. L. Giger, K. Doi, H. MacMahon, C. E. Metz, and F. F. Yin, ''Pulmonary nodules: computer-aided detection in digital chest image,'' RadioGraphics **10**, 41–51 (1990).
[6] T. Matsumoto, H. Yoshimura, K. Doi, M. L. Giger, A. Kano, H. MacMahon, K. Abe, and S. M. Montner, ''Image feature analysis of false-positive diagnoses produced by automated detection of lung nodules,'' Invest. Radiol. **27**, 587–597 (1992).
[7] Y. C. Wu, K. Doi, M. L. Giger, C. E. Metz, and W. Zhang, ''Reduction of false positives in computerized detection of lung nodules in chest radiographs using artificial neural networks, discriminant analysis and a rule-based scheme,'' J. Digital Imag. **7**, 196–207 (1994).
[8] T. Kobayashi, X. W. Xu, H. MacMahon, C. E. Metz, and K. Doi, ''Effect of a computer-aided diagnosis scheme on radiologists' performance in detection of lung nodules on radiographs,'' Radiology **199**, 843–848 (1996).
[9] X. W. Xu, K. Doi, T. Kobayashi, H. MacMahon, and M. L. Giger, ''Development of an improved CAD scheme for automated detection of lung nodules in digital chest images,'' Med. Phys. **24**, 1395–1403 (1997).
[10] J. Shiraishi, S. Katsuragawa, J. Ikezoe, T. Kobayashi, K. Komatsu, M. Matsui, H. Fujita, Y. Kodera, and K. Doi, ''Development of a digital image database for chest radiographs with and without a lung nodule: Receiver operating characteristic analysis of radiologists' detection of pulmonary nodules,'' Am. J. Roentgenol. **174**, 71–74 (2000).
[11] X. W. Xu and K. Doi, ''Image feature analysis for computer-aided diagnosis: Accurate determination of ribcage boundary in chest radiographs,'' Med. Phys. **22**, 617–626 (1995).
[12] X. W. Xu and K. Doi, ''Image feature analysis for computer-aided diagnosis: Detection of right and left hemidiaphragm edges and delineation of lung field in chest radiographs,'' Med. Phys. **23**, 1613–1624 (1996).